BBA - Molecular Cell Research 1864 (2017) 1785–1798

Contents lists available at ScienceDirect

BBA - Molecular Cell Research

journal homepage: www.elsevier.com/locate/bbamcr

NF-κB p65 serine 467 phosphorylation sensitizes mice to weight gain and TNFα-or diet-induced inflammation

Tabea Riedlinger[a,1], Marleen B. Dommerholt[b,1], Tobias Wijshake[c,d,1], Janine K. Kruit[b], Nicolette Huijkman[c], Daphne Dekker[c], Mirjam Koster[c], Niels Kloosterhuis[c], Debby P.Y. Koonen[c], Alain de Bruin[c,f], Darren Baker[d,e], Marten H. Hofker[c,2], Jan van Deursen[d,e], Johan W. Jonker[b], M. Lienhard Schmitz[a,1], Bart van de Sluis[c,*,1]

[a] Institute of Biochemistry, Medical Faculty, Friedrichstrasse 24, Justus-Liebig-University, D-35392 Giessen, Germany
[b] Section of Molecular Metabolism and Nutrition, Department of Pediatrics, University of Groningen, University Medical Center Groningen, Antonius Deusinglaan 1, 9713, AV, Groningen, The Netherlands
[c] Section of Molecular Genetics, Department of Pediatrics, University of Groningen, University Medical Center Groningen, Antonius Deusinglaan 1, 9713, AV, Groningen, The Netherlands
[d] Departments of Pediatrics and Adolescent Medicine, Mayo Clinic College of Medicine, Mayo Clinic, 200 First Street Southwest, Rochester, MN, USA
[e] Department of Biochemistry and Molecular Biology, Mayo Clinic College of Medicine, Mayo Clinic, 200 First Street Southwest, Rochester, MN, USA
[f] Dutch Molecular Pathology Center, Department of Pathobiology, Faculty of Veterinary Medicine, Utrecht University, Utrecht, The Netherlands

ARTICLE INFO

Keywords:
Metabolism
Inflammation
Gene expression
Aging
Insulin
Obesity

ABSTRACT

The NF-κB family of transcription factors is essential for an effective immune response, but also controls cell metabolism, proliferation and apoptosis. Its broad relevance and the high connectivity to diverse signaling pathways require a tight control of NF-κB activity. To investigate the control of NF-κB activity by phosphorylation of the NF-κB p65 subunit, we generated a knock-in mouse model in which serine 467 (the mouse homolog of human p65 serine 468) was replaced with a non-phosphorylatable alanine (S467A). This substitution caused reduced p65 protein synthesis and diminished TNFα-induced expression of a selected group of NF-κB-dependent genes. Intriguingly, high-fat fed S467A mice displayed increased locomotor activity and energy expenditure, which coincided with a reduced body weight gain. Although glucose metabolism or insulin sensitivity was not improved, diet-induced liver inflammation was diminished in S467A mice. Altogether, this study demonstrates that phosphorylation of p65 serine 467 augment NF-κB activity and exacerbates various deleterious effects of overnutrition in mice.

1. Introduction

The NF-κB family of transcription factors plays a critical role in numerous biological processes such as inflammation, cell survival, and metabolism by regulating a wide array of genes [1,2]. Sustained NF-κB activity has been implicated in a variety of diseases, including metabolic and immunological disorders, cancer, aging, and age-related diseases [3–6], indicating the necessity for a specific and precise control of NF-κB-mediated transcription. The NF-κB family consists of five DNA-binding subunits, namely p65 (*RelA*), p50 (*NFKB1*), p52 (*NFKB2*), c-Rel, and RelB which form homo- or heterodimers [2]. In the inactive state, the NF-κB DNA-binding subunits are maintained in the cytoplasm through association with inhibitory IκB proteins such as IκBα [7]. Exposure of cells to agents such as damage- or danger-associated molecular patterns or pathogen-associated patterns leads to the induction of signaling cascades resulting in NF-κB activation [8]. NF-κB activation via the canonical pathway is mediated by the IκB kinase (IKK) complex, which leads to the phosphorylation of IκBα and its subsequent degradation by the ubiquitin/proteasome system. This in turn enables the nuclear translocation of NF-κB where it can bind to cognate κB-sequences and activate transcription [9]. The termination of the NF-κB response is ensured by several negative feedback loops such as the NF-κB-dependent re-synthesis of IκBα, which enters the nucleus to remove the DNA-binding subunits from the DNA [10] and transfer them back into the cytoplasm via its nuclear export signal.

Each individual NF-κB activating stimulus induces an overlapping

* Corresponding author.
E-mail address: a.j.a.van.de.sluis@umcg.nl (B. van de Sluis).
[1] Equal contribution.
[2] Deceased.

http://dx.doi.org/10.1016/j.bbamcr.2017.07.005
Received 25 January 2017; Received in revised form 23 June 2017; Accepted 14 July 2017
Available online 16 July 2017

and distinct set of target genes with kinetics and amplitudes tailored to suit the specific requirements of the stimulus [11]. Gene-specific regulation of NF-κB activity is achieved by several mechanisms including posttranslational modification (PTM) of DNA-binding subunits such as the strongly transactivating p65 subunit [12–17]. Site-specific phosphorylation of p65 controls its conformation, protein/protein interactions, stability and transcriptional activity [15]. The p65 transactivation domain contains many constitutive and regulated phosphorylation sites, thus allowing to control NF-kB-mediated gene expression [8,15]. One of these p65 phosphorylation sites is serine 468 (S468). Basal phosphorylation of this site is mediated by glycogen synthase kinase 3 beta (GSK-3β), while inducible phosphorylation is mediated by IKKβ and IKKε [18–20]. It has been demonstrated that phosphorylation of p65 S468 contributes to selective termination of NF-κB dependent gene expression upon assisting in binding of an E3 ubiquitin ligase complex to p65. This multimeric ubiquitin ligase complex includes the components SOCS1, COMMD1, cullin 2 and the auxiliary factor GCN5 to mediate the ubiquitination and subsequent proteasomal-dependent removal of chromatin-bound p65 at promoter sites of a subset of NF-κB genes [21,22]. $p65^{-/-}$ MEFs reconstituted with a non-phosphorylatable p65 S468A mutant showed a small elevation of TNFα- or IL-1β-induced expression of a NF-κB-dependent reporter gene [20]. Consistent with this notion, the TNF-triggered expression of the NF-κB target genes *Icam1* and *Vcam1* were increased in MEFs expressing p65 S468A [23]. In contrast, another reporter gene study found reduced NF-κB activity for the p65 S468A mutant [19]. These inconsistent results highlight the need for a proper genetic model to study the importance and biological significance of p65 S468 phosphorylation for NF-κB function and activity *in vivo*. Here, we generated a knock-in mouse model in which p65 serine 467 (homologous to human p65 serine 468) was mutated to alanine. We demonstrate that TNFα-induced gene expression of selected NF-κB target genes is impaired due to reduced transcriptional activity of the mutant p65 protein. Absent p65 S467 phosphorylation abrogates the anti-apoptotic function of NF-κB in MEFs, and male mice expressing non-phosphorylatable p65 S467A mutant display reduced high-fat induced (HFD) liver inflammation, and body weight gain.

2. Results

2.1. Generation of p65 S467A knock-in mice

To assess the role of p65 S468 phosphorylation in NF-κB activity *in vivo* we generated a knock-in mouse in which serine 467 was substituted by alanine. Using homologous recombination in embryonic stem (ES) cells (Fig. 1A), we replaced the thymine with a guanine in the murine p65 encoding *p65* gene at position c.1399 resulting in a S467A allele (Fig. 1A). Chimeric mice were obtained by microinjection of correctly targeted ES clones into C57BL6/J blastocysts. These chimeras successfully transmitted the mutated *p65* allele (referred to as $p65^{NEO;S467A}$) to their offspring (Fig. 1B). $p65^{+/NEO;S467A}$ mice were crossed with *Hprt*-Cre transgenic mice [24] to excise the NEO gene cassette (Fig. 1A). Crosses between heterozygous $p65^{+/S467A}$ mice resulted in the generation of $p65^{S467A/S467A}$ (S467A) mice (Fig. 1C). Sequencing p65 cDNA of wild type and S467A mice confirmed the replacement of thymine into a guanine at position c.1399 (Fig. 1D). In contrast to *p65* knock-out mice, which are embryonically lethal [25], homozygous S467A knock-in mice were born at the expected Mendelian frequency (Fig. 1E), and were indistinguishable from control littermates at birth.

2.2. The p65 S467A mutation results in reduced p65 protein levels

To investigate the role of p65 S467 phosphorylation in NF-κB-mediated transcription, we cultured MEFs from wild type and p65 S467A embryos (13.5 dpc). Western blot analysis of MEF lysates showed significantly reduced p65 protein levels in p65 S467A MEFs. Quantitation of p65 revealed that S467A MEFs have only one third of the p65 protein levels as compared to wild type MEFs (Fig. 2A). This reduction in p65 levels was detected with two different antibodies recognizing epitopes corresponding to different domains (C-terminus and N-terminus) of p65 (Fig. S1A), excluding that the observed p65 S467A reduction is caused by diminished affinity of the C-20 antibody for the p65 mutant. Levels of *p65* mRNA were only slightly lowered in S467A MEFs, indicating that the reduced p65 protein levels cannot be fully explained by impaired gene transcription (Fig. 2A). A reduction of p65 protein levels in S467A mice was also seen in tissue homogenates from various organs and was most prominent in the kidney, lung and gastrocnemius muscle (Fig. 2B,C). Expression analysis of *p65* mRNA in the different organs demonstrated a slight reduction of ~20% in S467A mice, but the difference was only statistically significant in kidney and heart (Fig. 2D).

As the reduction of p65 levels is not fully attributable to impaired gene expression, we further analyzed possible mechanisms responsible for decreased p65 protein levels. Protein synthesis was blocked with anisomycin and constitutive p65 decay was monitored over time. These experiments did not reveal a significant difference in the protein stabilities of p65 and p65 S467A under basal conditions (Fig. S1B). In line with this, no enhanced proteosomal and lysosomal degradation of p65 S457A was seen in MEFs (Fig. S1C). Also, *p65* mRNA stability was not affected in the S467A mutants compared to the controls, as seen after inhibition of RNA synthesis by actinomycin D (Fig. S1D). Intriguingly, however, *de novo* synthesized p65 in S467A MEFs was reduced compared to wild type MEFs, as determined by chase experiments with radiolabeled amino acids (Fig. 2E,F, Fig. S1E).

As NF-κB DNA binding subunits can mutually control their expression levels we also determined the relative abundance of other DNA-binding subunits in S467A MEFs. Although the levels of p105/p50, RelB, and c-Rel were not affected by the S467A mutation, the levels of p100/p52 levels were slightly reduced (Fig. S1F).

2.3. Phosphorylation of p65 S467 contributes to IκBα resynthesis and p65 nuclear export

We have previously observed a functional role of p65 S536 phosphorylation in the kinetics of p65 nuclear import [26], therefore we tested whether phosphorylation at S467 can affect this process. MEFs expressing p65 S467A and control MEFs were stimulated for various periods with TNFα and fractionated into cytosolic (C), nucleosolic (N1) and chromatin (N2) extracts. While TNF-triggered translocation of p65 to the nucleosolic and chromatin fractions was not affected by S467 phosphorylation, the re-export of nuclear p65 was slightly delayed in the p65 S467 expressing cells, as revealed by Western blot analysis (Fig. 3A,B). As nuclear export of NF-κB is mainly mediated by IκBα [27], we compared the IκBα degradation and resynthesis rates between MEFs expressing wild type p65 and the phospho-site mutant. Immunoblotting showed that TNFα-triggered degradation of the IκBα protein was fully comparable, but the re-synthesis rate of the IκBα protein was slower and less complete in p65 S467A expressing cells (Fig. 3C,D). Interestingly, this effect was not seen at the mRNA level at early time points (Fig. 3E), suggesting that p65 phosphorylation improves IκBα protein synthesis, which coincide with enhanced nuclear export of p65. Alternatively, the reduced protein levels of *de novo* synthesized IκBα might be a consequence of the diminished p65 amounts available for IκBα in S467A MEFs, as free IκBα is more instable than p65-bound IκBα [28].

We also determined p65 Ser534 phosphorylation (murine homolog of human p65 serine 536), which is a surrogate marker for IKK activity [29]. The TNFα-triggered p65 Ser534 phosphorylation in S467A cells was unchanged in relation to the total amount of p65 (Fig. 3C,D).

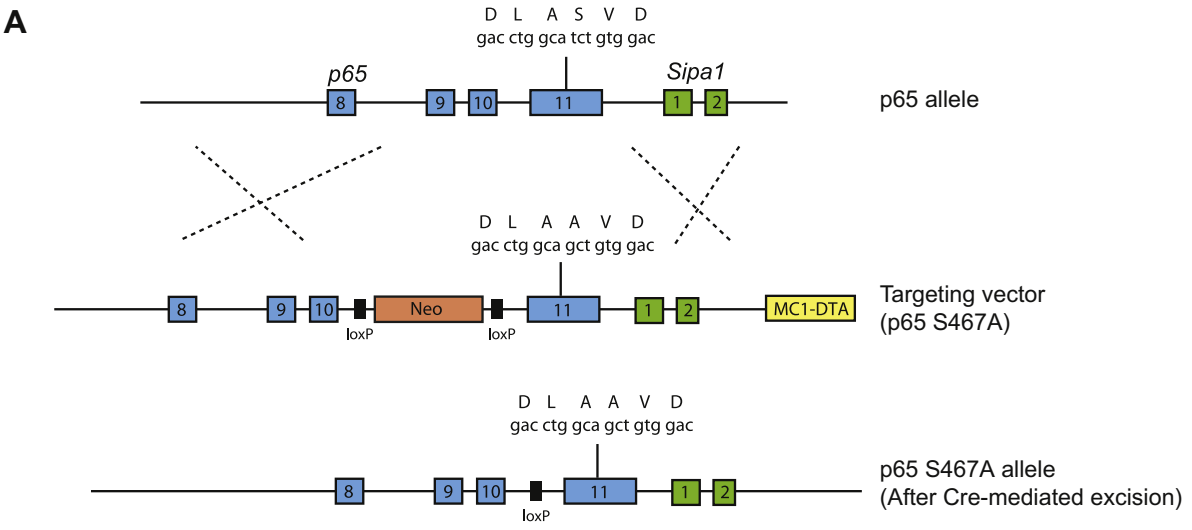

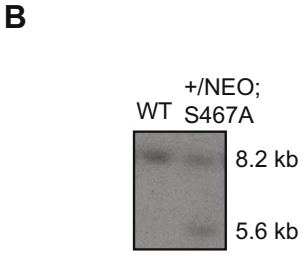

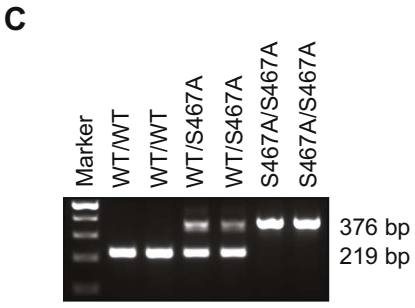

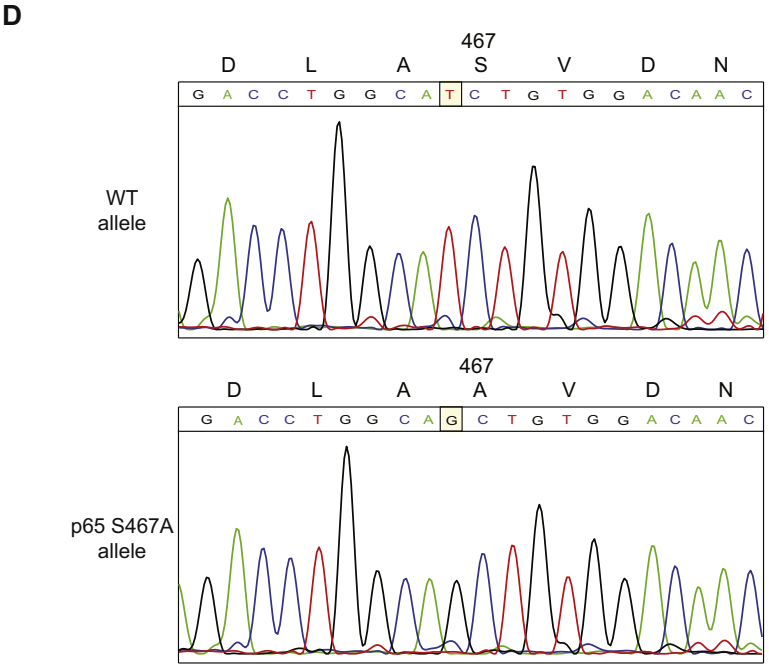

E

	Genotype			
	+/+	+/m	m/m	Total
Born	68	116	54	238
Expected	59.5	119	59.5	238

Fig. 1. Generation of *p65* S467A knock-in mice. (A) Gene targeting strategy to generate $p65^{S467A/S467A}$ mice. Indicated are the genomic mouse *p65* locus spanning exon 8–11 of *p65* and exon 1–2 of *Sipa1* (top); the targeting vector with the T > G substitution in exon 11 (red), loxP sites (black boxes); the *p65* S467A locus after targeted recombination and crossing with *Hprt*-Cre recombinase mice to remove the NEO cassette and produce $p65^{+/S467A}$ mice. (B) Southern blot of *Xba*I digested genomic DNA from two ES cell clones and probed with DNA fragment showing the 8.2 kb and 5.6 kb fragments representing the wild type and $p65^{NEO;S467A}$ allele, respectively. (C) PCR genotyping of DNA extracted from the tails of two wild type, two $p65^{+/S467A}$ and two $p65^{S467A/S467A}$ mice. (D) Sequencing of *p65* cDNA obtained by RT-PCR from livers of wild type and $p65^{S467A/S467A}$ mice. (E) Genotype analysis of offspring derived from breeding S467A heterozygous parents. The expected Mendelian frequency is indicated at the bottom.

2.4. Preventing phosphorylation of S467 impairs transactivation of NF-κB-target genes

Previous studies have demonstrated that phosphorylation of p65 has an essential role in the transcriptional output of NF-κB [19,20,30,31]. To determine whether the S467A mutation affects NF-κB-mediated transcription, we examined the inducible expression of a number of well-known NF-κB target genes. We stimulated both wild type and S467A MEFs with TNFα and monitored the expression kinetics of these genes by qRT-PCR. S467A MEFs showed impaired transactivation of various pro-inflammatory cytokines, such as *Tnfα, Il-1α*, and *Mcp-1*. No statistically significant changes were seen for the expression of *Il6* and

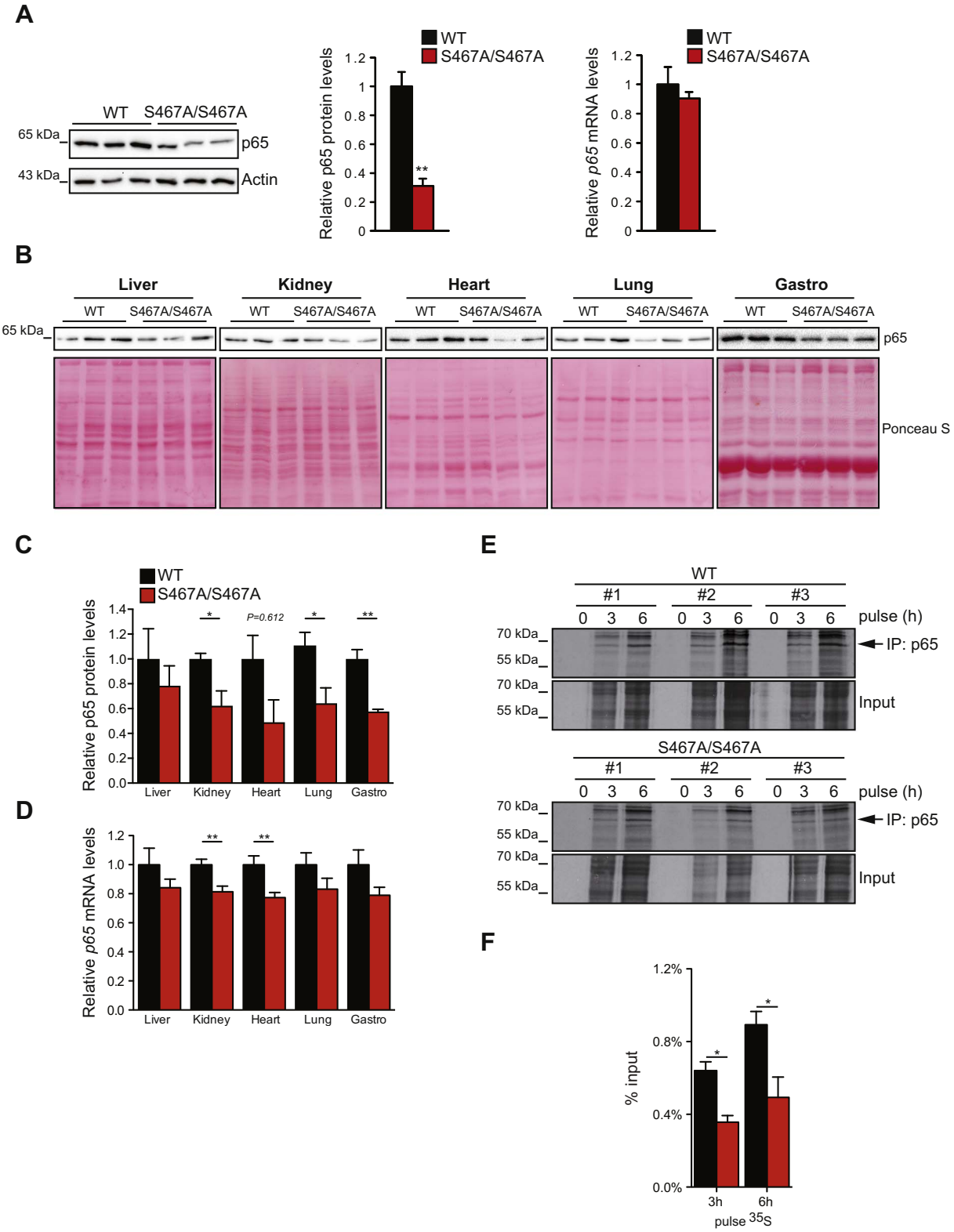

Fig. 2. Characterization of *p65* S467A mutant MEFs. (A) Immunoblot analysis of p65 protein levels in wild type and S467A MEFs generated from embryos at 13.5 dpc. Actin was used as a loading control (left). Quantitation of relative p65 protein amount in 3 independent wild type and homozygous knock-in MEF lines (middle). Relative *p65* mRNA expression of wild type ($n = 3$) and homozygous knock-in MEFs ($n = 3$) as determined by quantitative RT-PCR (right). All values represent average ± SEM, ** = $P < 0.01$. (B) Western blot analysis of p65 protein levels in various tissues of 3-month-old male wild type and homozygous knock-in mice. Ponceau S staining was used as a loading control. Gastro = gastrocnemius muscle. (C) Quantitative analysis of p65 protein amounts in different organs (Fig. 2B). (D) Quantitative analysis of *p65* mRNAs isolated from different organs from wild type ($n = 7$) and knock-in ($n = 7$) animals. (E) Wild type and S467A MEFs were incubated with ^{35}S–labelled cysteine and methionine for the indicated periods. One fraction of the total lysate was used as an input control while another fraction was used to immunoprecipitate p65 with specific antibodies. The material was analyzed by SDS-PAGE and autoradiography, the arrow points to the immunoprecipitated p65 protein. (F) Quantification of fig. (E). Values for immunoprecipitated p65 were normalized to the input. All values represent average ± SEM, * = $P < 0.05$.

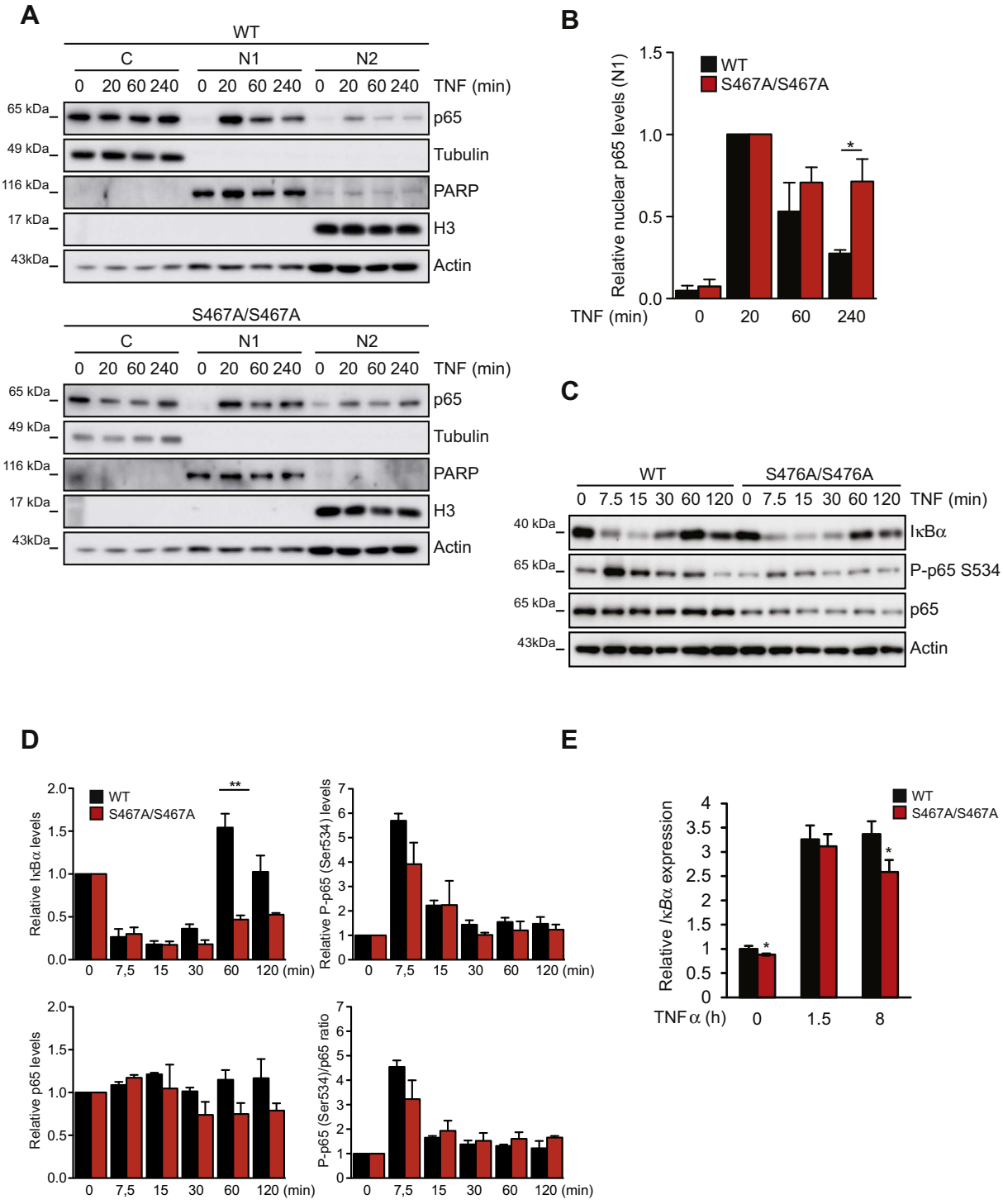

Fig. 3. NF-κB p65 S467 phosphorylation contributes to efficient IκBα protein resynthesis and nuclear export of p65. (A) MEFs from wild type animals and knock-in mice were treated for the indicated periods with TNFα and cells were fractionated into the cytosolic (C), soluble nuclear (N1) and insoluble nuclear (N2) fraction. These fractions were analyzed for the kinetics of p65 nuclear import and export by immunoblotting. The purity of the fractions was controlled by blotting for Tubulin (C), PARP (N1) and histone H3 (N2). (B) Quantitative analysis of p65 protein amounts in the N1 fraction from three independent experiments, normalized to PARP expression. (C) Western blot analysis of degradation and resynthesis of IκBα proteins in whole cell extracts of MEFs after TNFα stimulation (10 ng/ml). In addition, the levels of serine 534 phosphorylated p65 in wild type and $p65^{S467A/S467A}$ MEFs are indicated. (D) The levels of the indicated proteins from the experiment displayed in (C) and two further experiments were quantified. (E) The indicated MEFs ($n = 6$ for both genotypes) were stimulated for 1, 5 or 8 h with TNFα and *IκBα* mRNA levels were determined by qRT-PCT. All values represent average ± SEM, * = $P < 0.05$, ** = $P < 0.01$.

Saa3 (Fig. 4A). In addition, the gene expression of two cell adhesion molecules, *Icam1* and *Vcam1* was markedly reduced in S467A MEFs (Fig. 4A).

To assess whether aberrant binding of p65 to promoter/enhancer regions causes these differences in gene expression we performed chromatin immunoprecipiation (ChIP) assays. TNFα treatment enhanced the binding of p65 to known NF-κB binding sites in the promoter of *Icam1* and *Vcam1* in wild type and S467A MEFs (Fig. 4B). Although no differences in association of p65 to the *Icam1* promoter were seen, the abundance of p65 to its binding site at the *Vcam1* gene was significantly higher in S467A MEFs after 8 h of TNFα stimulation (Fig. 4B).

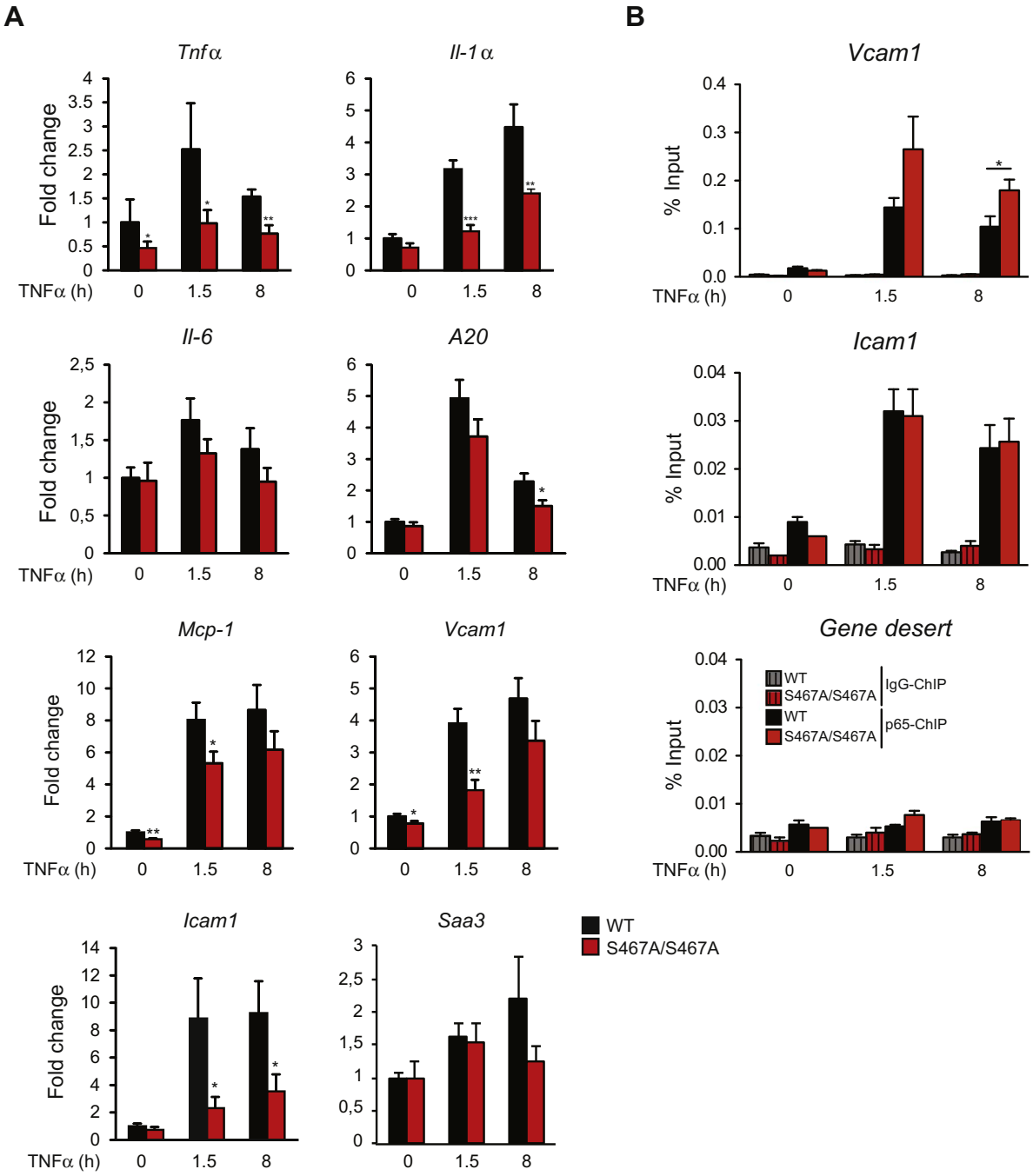

Fig. 4. Diminished NF-κB-mediated gene expression by the loss of p65 S467 phosphorylation is not due to impaired DNA-binding of p65. (A) Relative mRNA expression of pro-inflammatory cytokines and NF-κB target genes at 0, 1, 5 and 8 h after TNFα stimulation (10 ng/ml). Values represent 6 independent wild type and S467A MEF lines. (B) MEFs from wild type controls ($n = 3$) or from p65 S467A ($n = 3$) animals were treated for 1, 5 or 8 h with TNFα. Chromatin was immunoprecipitated with antibodies recognizing p65 NF-κB or a control IgG, followed by qPCR analysis of the retrieved DNA regions representing known NF-κB binding sites at the *Icam1* and *Vcam1* enhancers/promoters or a gene desert as a control. Mean values of three independent experiments are shown. All values represent average ± SEM, * = $P < 0.05$, ** = $P < 0.01$.

The reduced expression of many NF-κB target genes might be explained by a stimulatory role of S467 phosphorylation, but may be also due to the lower p65 protein expression level observed in the knock-in cells. To distinguish between these two possibilities, we also measured gene expression in $p65^{+/-}$ MEFs that express reduced levels of p65 protein (~55% compared to wild type) (Fig. S2). Basal and TNFα-induced expression of several NF-κB target genes (e.g. *Ikbα*, *A20*, *Mcp1* and *Vcam1*) in $p65^{+/-}$ MEFs was in many cases much stronger reduced then in S467A cells compared to control cells (Fig. S2, Fig. 4A).

Next, we evaluated whether the S467A mutation affects the activation of NF-κB *in vivo*. Wild type and S467A mutant mice received an injection of either TNFα or PBS and the expression of various NF-κB genes was examined by qRT-PCR. Analysis of a number of tissues at 1 h post injection revealed markedly reduced *Icam1* expression in liver, kidney, heart, lung and gastrocnemius muscle of S467A mice (Fig. 5). Furthermore, the induced expression of the inflammatory cytokines *Mcp1* and *Tnfα* was impaired in most tissues of S467A mutant mice. TNF-induced expression of *Il-6* was impaired in most organs except the liver (Fig. 5).

Taken together, these data demonstrate that loss of p65 S467 phosphorylation impairs the transactivation of a subset of NF-κB target genes, which can not entirely explained by reduced p65 protein levels,

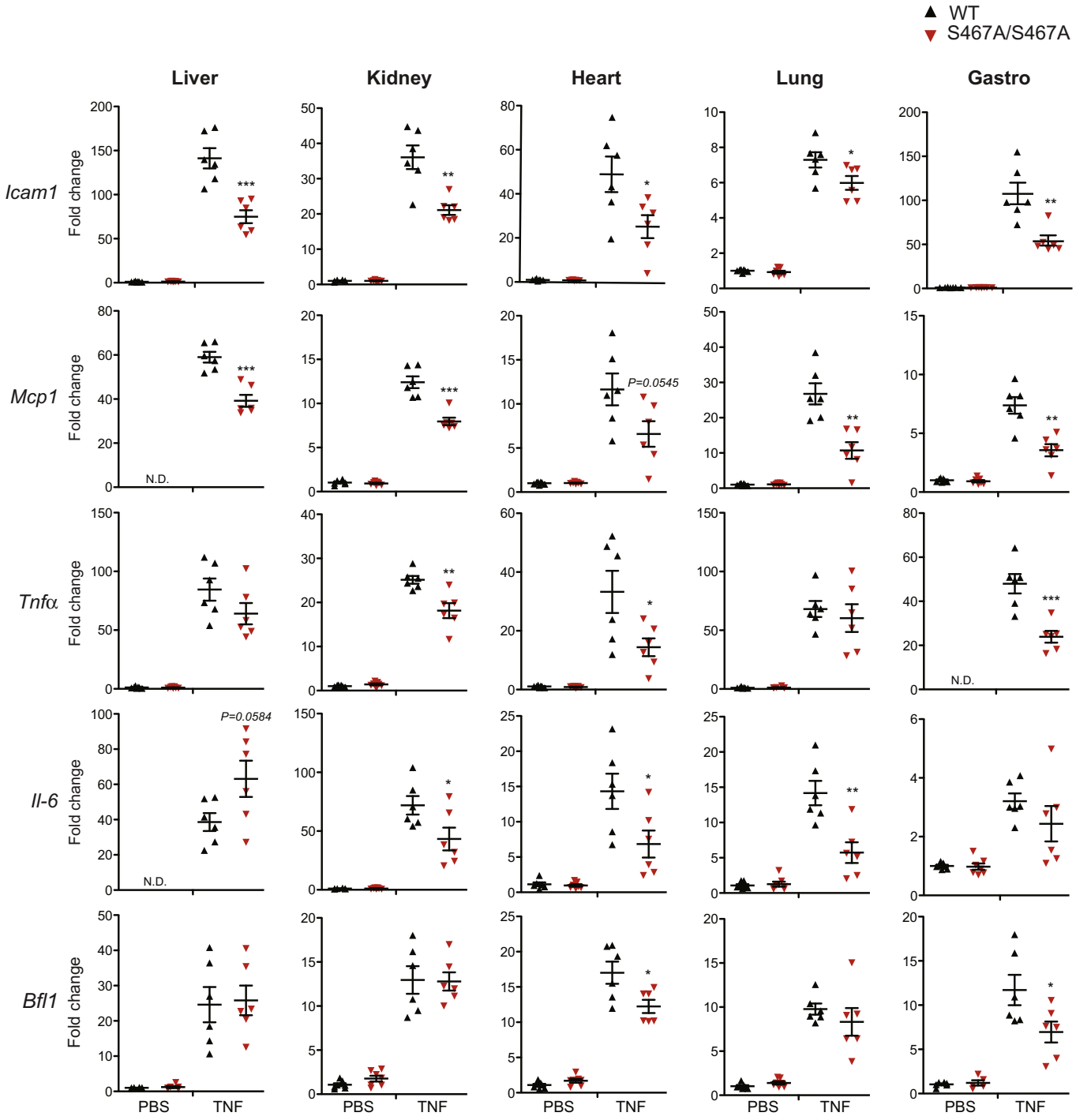

Fig. 5. Preventing p65 S467 phosphorylation attenuates NF-κB-mediated gene expression. Expression of pro-inflammatory and NF-κB target genes was assessed in various tissues at 1 h after injection with either PBS ($n = 7$ for both genotypes) or TNFα (15 μg/kg) ($n = 6$ for both genotypes). All values represent average ± SEM, * = $P < 0.05$, ** = $P < 0.01$, and *** = $P < 0.001$.

nor by impaired p65 binding to known κB-sequences.

2.5. S467A MEFs are sensitive to TNFα-induced apoptosis

As p65-deficient mice are sensitive to TNF-triggered apoptosis [16,25,32], we examined the role of S467A phosphorylation for TNFα-induced cell death. MEFs were exposed to various concentrations of TNFα and cell viability was compared between wild type and p65 S467A MEFs. These experiments revealed an increased sensitivity of p65 S467 MEFs to TNFα (Fig. 6A). In contrast, *p65* haplo-insufficient MEFs showed no significant increased sensitivity to TNFα-induced cell death, when compared to wild type controls (Fig. 6A), indicating that the level of p65 protein is not responsible for the difference in apoptosis. To further investigate the effect of p65 S467A on apoptosis, we determined TNF-induced caspase activity. For this, cells were exposed to different concentrations of TNFα and cleavage of the caspase substrate ADP-ribose polymerase (PARP) was measured by immunoblotting. Western blot experiments showed a marked increase in TNFα-triggered caspase activity in p65 S467A cells (Fig. 6B). This elevated sensitivity to TNFα was accompanied by decreased expression of NF-κB-

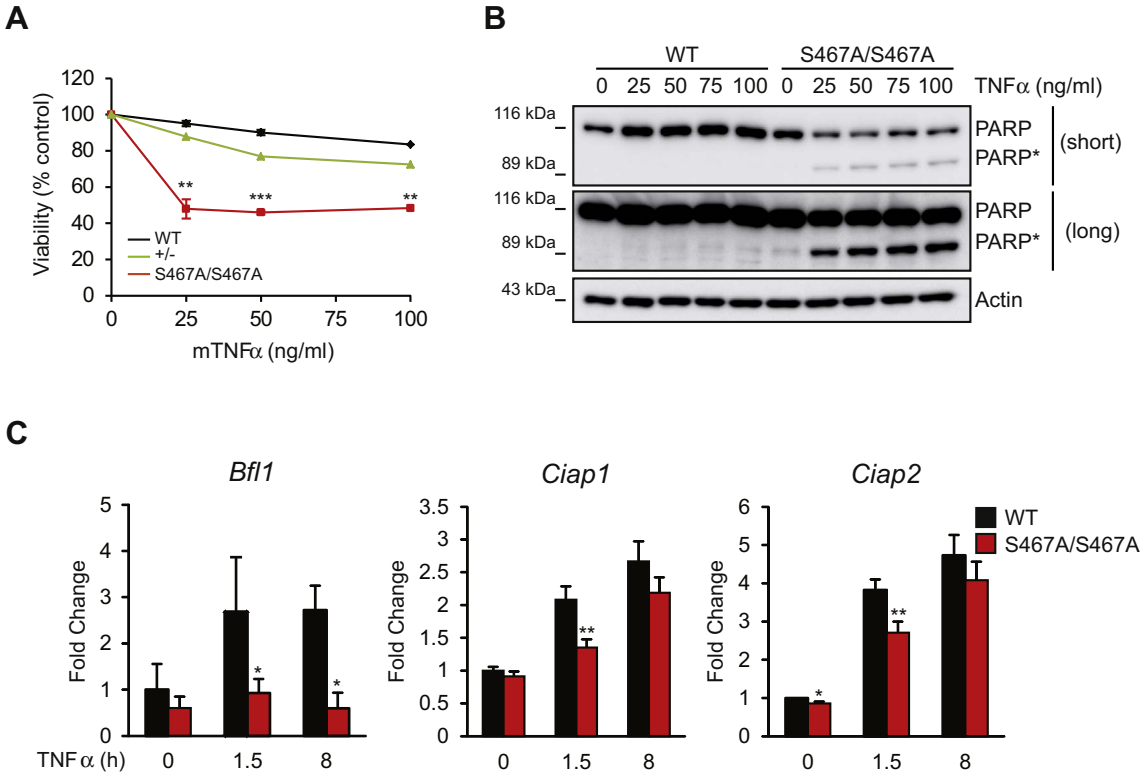

Fig. 6. p65 S467 phosphorylation contributes to the anti-apoptotic function of NF-κB. (A) Cell viability was assessed in wild type, p65 S467A, and $p65^{+/-}$ MEFs after 24 h exposure to various amounts of TNFα, 3 independent MEF lines were used, in case of $p65^{+/-}$ only one cell line was used. (B) Wild type and p65 S467A MEFs were treated for 24 h with various amounts of TNFα. Caspase activity was determined upon detection of the cleavage of the caspase substrate protein PARP to the 85 kDa cleavage product (indicated as PARP*). (C) MEFs from wild type controls and p65 S467A knock-in animals were treated for 1, 5 or 8 h with TNFα and the expression of NF-κB-dependent anti-apoptotic genes was quantified by qRT-PCR. All values represent average ± SEM, * = $P < 0.05$, and ** = $P < 0.01$.

mediated anti-apoptotic genes (Fig. 6C). These data suggest that p65 S467 phosphorylation is important to protect MEFs against TNFα-induced apoptosis.

2.6. Male p65 S467 mice are protected against diet-induced obesity

Homozygous p65 S467A mice were born at the expected Mendelian frequency (Fig. 1E), were healthy and did not display any obvious phenotypic abnormalities. Histological analysis of liver, kidney and spleen did not reveal any substantial differences in adult male mice (Fig. S3). Also the relative weight of these organs (Fig. S4) and the number of white and red bloods cells were unaffected in S467A mice (Table 1). When we compared the body weight gain in adolescent animals, however, we noted a tendency for reduced weight gain and plasma triglycerides levels in p65 knock-in male mice (Fig. 7A, Table 1). At one year of age, the reduced weight gain was statistically significant in male mice (Fig. 7B).

The reduced body weight gain in male S467A mice suggests a role for basal p65 S467 phosphorylation in metabolic regulation. Of note, the kinases IKKβ, IKKε, and GSK-3, which are known to phosphorylate p65 at serine 467 have been implicated in the regulation of weight gain, diet-induced obesity, and insulin resistance [33–37]. Therefore, we examined whether p65 S467 phosphorylation plays a role in diet-induced obesity, insulin sensitivity and tissue inflammation. Wild type and S467A male mice were challenged with a 60% high fat diet (HFD) for 12 weeks. After 6 weeks of HFD feeding, S467A mice gained significantly less weight and this difference remained until the end of the experiment (Fig. 7C). MRI and weight analysis of different adipose tissues indicated that this reduced weight gain was partly due to reduced subcutaneous white adipose tissue (scWAT), as interscapular brown adipose tissue (iBAT) and lean mass did not differ between wild type and S467A mice (Fig. 7D, E). As body weight gain represents an imbalance of food intake and energy expenditure, we assessed whether they were affected by phosphorylation of p65 S467. No differences between the groups were observed for food intake (Fig. 7F), content of calories, neutral sterols and bile acid in the feces (Fig. S5A-C). However, the locomotor activity and energy expenditure of S467A mice were significantly elevated compared to wild type mice (Fig. 7G, H). O_2 consumption per kg of body weight was slightly increased, both in the light and dark phase (Fig. S5D). We also compared the respiratory quotient (RQ = VCO_2/VO_2) (Fig. S5E), but no differences between genotypes were seen. Previously it has been suggested that energy expenditure can be increased secondary due to increased thermogenesis [36], and thus the mRNA levels of the uncoupling proteins UCP1 and UCP2 were determined. However, no differences in the *Ucp1* and *Ucp2* mRNA levels in white adipose (epididymal) tissue of wild type and S467A mice were seen (Fig. S6).

Although diet-induced body weight gain in S467A mice was reduced, glucose tolerance and insulin sensitivity were not different

Table 1
Parameters of wild-type and homozygous S467A male mice (23 wks of age).

Parameters	wild type	S467A	*P* value
Body weight (g)	35.58 ± 0.82	33.71 ± 1.26	0.22
Weight gain (g)	4.69 ± 0.5	3.48 ± 0.78	0.19
Glucose (mM)	9.96 ± 0.3	10.25 ± 0.48	0.6
Insulin (ng/ml)	0.61 ± 0.11	0.5 ± 0.04	0.37
Triglyceride (mM)	0.46 ± 0.054	0.30 ± 0.0142	0.018*
Cholesterol (mM)	3.08 ± 0.065	2.87 ± 0.097	0.076
Blood counts (RB) (10*9/ml)	9.46 ± 0.14	9.36 ± 0.07	0.56
Blood counts (WC) (10 * 6/ml)	7.74 ± 0.7	6.69 ± 0.73	0.31

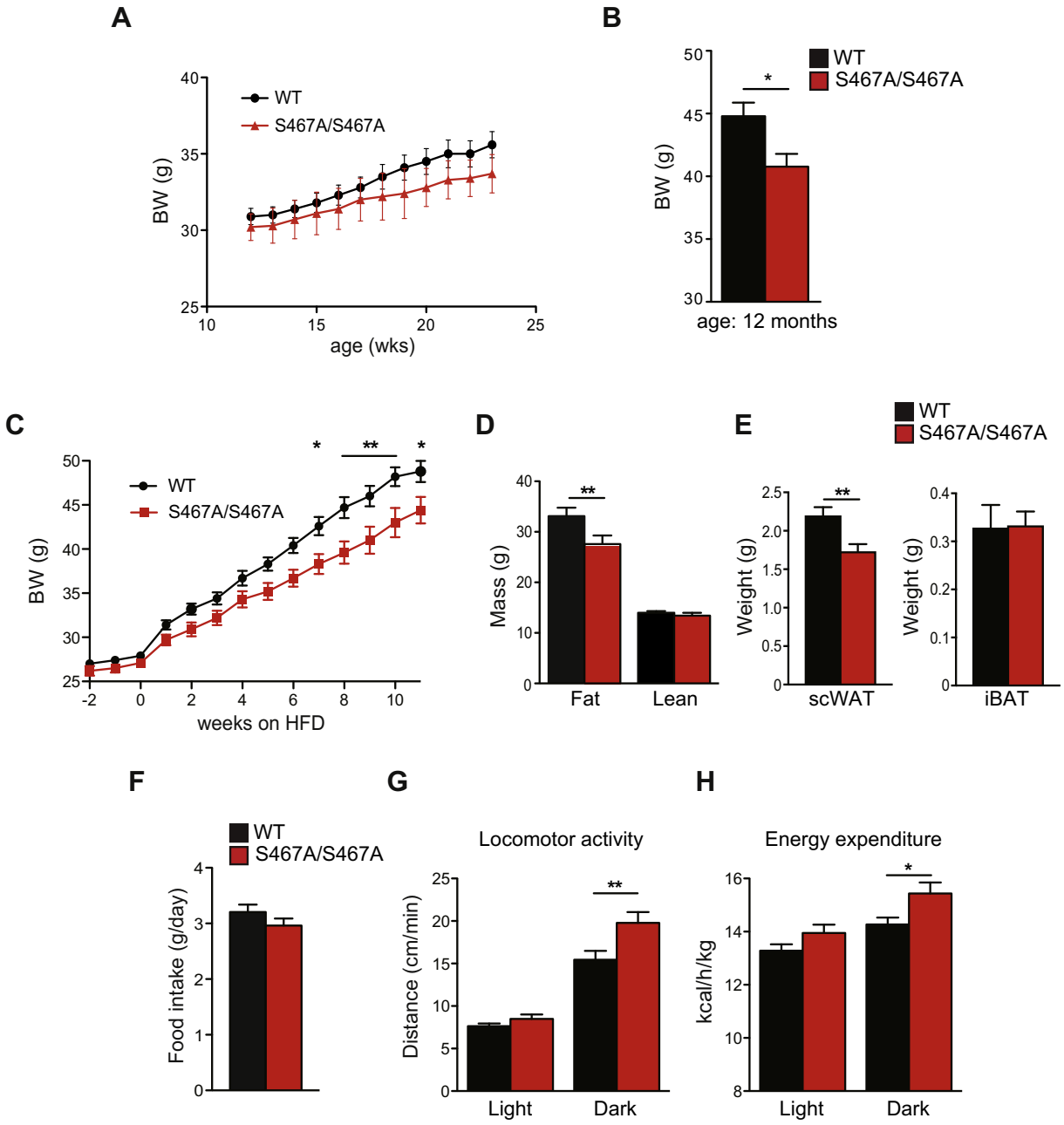

Fig. 7. Increased locomotor activity is associated with decreased weight gain in male p65 S467A mice. (A) Starting at 12 weeks of age the total body weight of wild type mice ($n = 8$) and p65 S467A male mice ($n = 9$) was determined. (B) Body weight of male mice at 12 months of age ($n = 7$–13). (C) Body weights of male mice fed a HFD, starting at 10 weeks of age (wild type $n = 8$, S467A $n = 9$). (D) Fat and lean mass and (E) subcutaneous white adipose tissue (scWAT) and interscapular brown adipose tissues (iBAT) of wild type and S467A mice after 10 weeks of HFD feeding (wild type $n = 8$, S467A $n = 9$). (F) Average food intake during high fat feeding ($n = 8$–9), (G) locomotor activity, (H) energy expenditure (8 mice per genotype). All values represent average ± SEM, * = $P < 0.05$, ** = $P < 0.01$, and *** = $P < 0.001$.

between genotypes (Fig. S7A, B). Obesity is associated with chronic low-grade inflammation in adipose tissue and liver, therefore, we evaluated the level of inflammation in both tissues after 12 weeks of HFD-feeding. Compromised p65 S467 phosphorylation did not reduce adipose tissue inflammation (Fig. S7C), but it significantly attenuated expression of inflammatory genes and inflammation in the liver (Fig. 8A, B). The liver weight and the accumulation of lipids of S467A mice were not significantly different (Fig. 8C, Fig. S8).

Altogether, a lack of p65 S467 phosphorylation increases locomotor activity leading to enhanced energy expenditure, which ameliorates comorbidities in diet-induced obese mice, such as weight gain and liver inflammation.

3. Discussion

The importance of several p65 PTMs in transcriptional regulation and physiology has been illustrated in various mouse models [30,38,39]. PTMs regulate the activity of NF-κB, which are essential in determining the duration and strength of nuclear NF-κB-mediated transcription [15]. Using a p65 mutant mouse with a nonphosphorylatable serine 467, we demonstrate that phosphorylation of p65 S467 is required for proper activation of NF-κB. We further show that a deficiency in S467 phosphorylation results in reduced p65 levels in MEFs and various tissues and diminished TNFα-induced expression of a subset of NF-κB-regulated genes. The attenuated NF-κB transactivation might be partly due to reduced p65 protein levels in S467A cells/tissues, but it does not fully explain the difference in gene expression

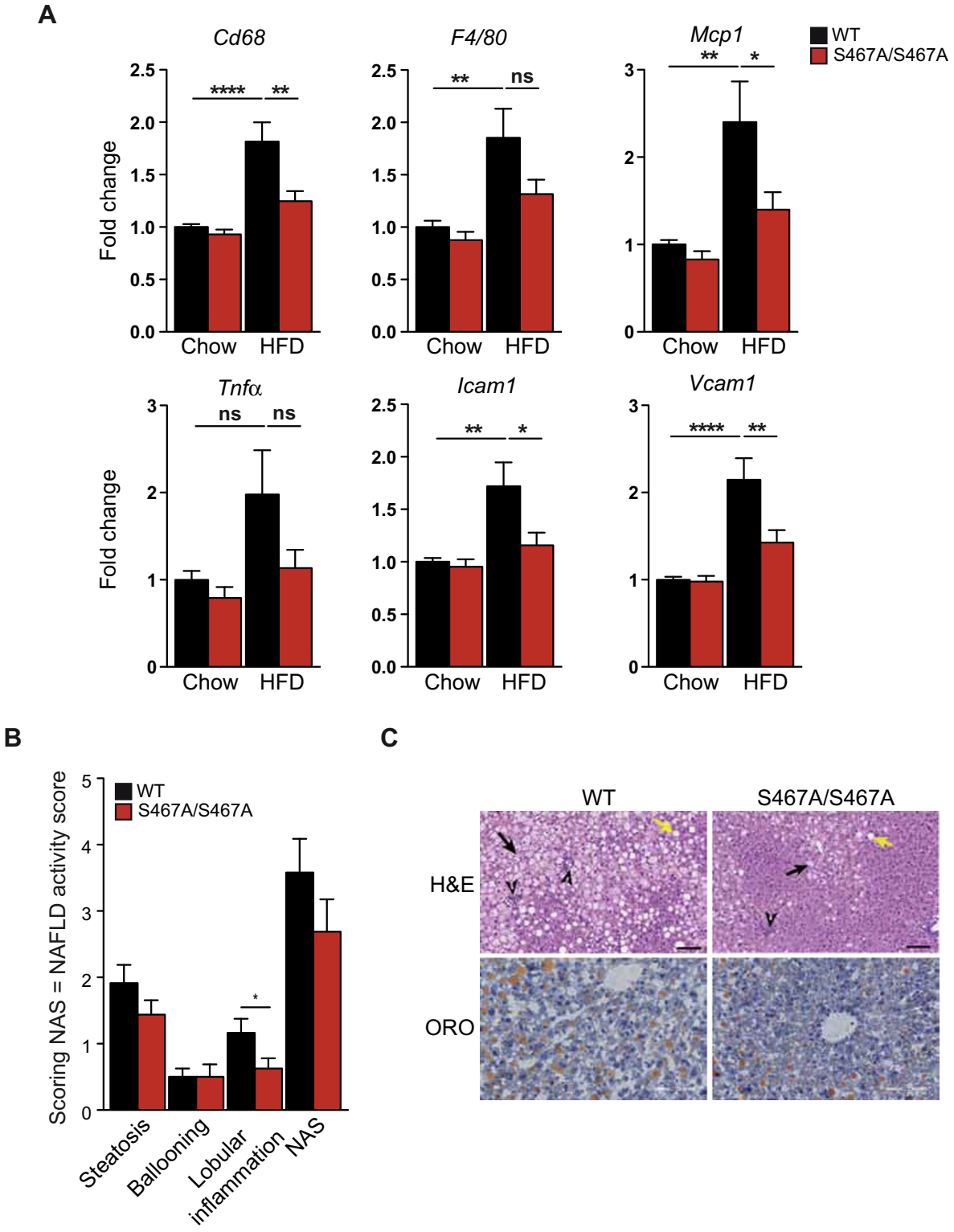

Fig. 8. Diet-induced expression of inflammatory genes is attenuated in the livers of male p65 S467A mice. (A) Relative mRNA expression of macrophage markers, pro-inflammatory cytokines and adhesion molecules in livers of chow (n = 8 mice per group) and 12 weeks HFD-fed wild type (n = 8) and S467A (n = 9) mice. (B) Pathological activity score for NALFD (NAS = steatosis + ballooning + lobular inflammation). (C) Representative pictures from H & E staining and Oil-red O staining of liver sections of wild type and p65 S467A mice fed a HFD (12 weeks) (bar represents 100 μM). Arrowheads point to inflammatory foci, black arrows point to microvesicular steatosis, yellow point to macrosteatosis. All values represent average ± SEM, * = $P < 0.05$, ** = $P < 0.01$, *** = $P < 0.001$, and **** = $P < 0.0001$.

response for a number of reasons. First, the expression of some NF-κB genes was unaffected in S467A MEFs, whereas these were markedly impaired in haplo-insufficient MEFs ($p65^{+/-}$). Second, the levels of reduction in TNF-induced NF-κB-mediated gene expression were larger in $p65^{+/-}$ MEFs. Finally, the level and residence time of p65 bound to the promoter of NF-κB-dependent genes were similar or even prolonged in S467A MEFs compared to wild type cells. Since the nuclear translocation of p65 and the level of DNA bound p65 are not adversely affected in S467A MEFs, implicate that p65 S467 phosphorylation is important for the interaction of p65 with co-regulatory proteins or

further PTMs, which are needed for optimal transactivation of a subset of NF-κB target genes [15,30,40].

The increased residence time of p65 S467A in the nucleus and at the promoter regions of NF-κB dependent genes, such as *Vcam1*, is in line with the previously described role of S467 phosphorylation in ubiquitin/proteasomal-dependent elimination of p65 from specific promoters [21,22]. However, here we demonstrate that p65 S467 phosphorylation is required for proper NF-κB activation, which is in contrast to previous work that shows that p65 S467 phosphorylation restrain NF-κB-controlled gene expression [21,22].

This study does not provide evidence for a role of p65 S467 phosphorylation in the proteasomal degradation of total p65 [21,22]. The conflicting results between this study and previous work might be explained by the different models used. Previous experiments used immortalized p65 null MEFs that were reconstituted with a plasmid containing only the coding region of human *p65* S468A, which resulted in relatively high p65 levels, which might be not physiological. Also, these plasmids do not express the full length p65 encoding mRNAs, which often contain regulatory elements in their 3′ends that control their translation efficiency [41].

Using cells derived from *p65* S467A mice in which the endogenous *p65* gene was genetically modified, we found that p65 S467 phosphorylation contributes to appropriate *de novo* synthesis of the p65 protein. Whether this is intrinsic to the mutant protein itself or an extrinsic effect that is caused by the loss of p65 S467 phosphorylation needs to be investigated in future studies. Thus, a decrease in *de novo* synthesis of p65 in combination with a slightly diminished *p65* gene expression likely explains the reduced p65 protein amounts in S467A MEFs and different tissues of S467A mice.

Here we found that preventing p65 S467 phosphorylation sensitized MEFs to TNFα-induced apoptosis, raising the possibility that S468 phosphorylation is of more general relevance for the anti-apoptotic effects of NF-κB. This is supported by prior work, showing that MEFs stably reconstituted with a human p65 S468A protein are more susceptible to cell death triggered by the DNA damaging agent etoposide [42].

Although S467A mice are born without an overt phenotype, middle-aged male mice have a lower body weight as compared to wild type littermates on chow diet. A reduced body weight gain was also observed upon HFD-feeding, which arose from increased locomotor activity and energy expenditure of S467A mice. The NF-κB activation pathway has an important biological role in the brain [43] and also affects pathways controlling energy consumption and obesity [35]. Overnutrition induces NF-κB activity in the hypothalamus, and genetic activation of the NF-κB pathway by IKKβ, a kinase that can also phosphorylate p65 at serine 467 [20], results in leptin resistance [35]. Since leptin resistance causes reduced locomotor activity and energy expenditure leading mice to gain weight [44–47], it is therefore tempting to speculate that NF-κB activity in the brain of S467A mice is reduced. This model would imply that p65 S467 phosphorylation contributes to diet-induced NF-κB activity in neurons and thereby negatively affects leptin sensitivity. Alternatively, differences in body-weight gain and locomotor activity between S467A mice and wild type littermates could be explained by genetic variations from the donor strain (129Sv/E) around the introduced mutation, also referred to as passenger genes effect [48]. We consider this possibility to be very unlikely, as the web tool “Me-Pa-MuFind-It” (http://me-pamufind-it.org) did not reveal any potential passenger mutation in 129-derived transgenic mice that may explain the phenotypic differences between wild type and mutant mice.

HFD-induced obesity is associated with chronic low-grade inflammation accompanied by insulin resistance [49,50]. In addition, overnutrition induces NF-κB activity through increased expression and activity of IKKε in adipose tissue and liver [36], likely also via phosphorylation of serine 467 of p65 [23]. Interestingly, improvement of some deleterious effects of HFD-feeding has been observed both in S467A and in IKKε knock-out (KO) mice [36]. IKKε KO mice are resistant to HFD-induced weight gain, insulin insensitivity, steatosis, and inflammation in liver and fat, whereas preventing p65 S467 phosphorylation only ameliorates weight gain and liver inflammation. Protection against insulin sensitivity was also seen in various models in which IKKβ was genetically or pharmaceutically targeted [33–35,51,52]. Although p65 S467 is a target of both IKKε and IKKβ, the relative mild protective effect by the loss of S467 phosphorylation in S467A mice might be explained by the fact that in addition to S467 many other residues in p65 and other proteins can be phosphorylated by the IKKs [53,54].

Recent studies demonstrated that low-grade liver inflammation does not significantly contribute to systemic insulin resistance [55,56]. Our results support these findings, as the reduced diet-induced liver inflammation in S467A mice did not improve systemic glucose tolerance and insulin resistance. Despite the reduced fat mass in S467A mice, the level of inflammation in adipose tissue was identical in both genotypes, underscoring the direct link between adipose tissue inflammation and systemic insulin resistance [56,57].

Collectively, we demonstrate that phosphorylation of p65 S467 positively contributes to selective NF-κB-mediated gene expression. Preventing p65 S467 phosphorylation diminishes the inflammatory response, and improves various adverse effects in diet-induced obese mice. Therefore, pharmacological interference with p65 S467 phosphorylation might be an interesting therapeutic strategy [58] to selectively attenuate the progression of inflammatory diseases.

4. Material and methods

4.1. Generation of S467A mice

The $p65^{S467A}$ allele was produced through recombineering as described before [59]. The genomic *p65* gene fragment spanning exons 8–11 was retrieved from BAC #bMQ-331N14 (129S7/SvEv ES Cell, Source BioScience) and transferred into pDTA.4B. Exon 11 was amplified with the following primers: forward (5′-AAGCTTTATGACCGCAGT-AGCTAG-3′) and reverse (5′-AAGCTTTAGTGGAAGCCCTGT-CCTAG-3′) and cloned into pZero (Invitrogen). Introduction of the S467A knock-in mutation into exon 11 was accomplished by site-directed mutagenesis using the following primers: forward (5′-GTTCACAGACCTGGCAGCT-GTGGACAACTCAGA-3′) and reverse (5′-TCTGAGTTGTCCACAGCTGC-CAGGTCTGTGAAC-3′). The mutated exon 11 was amplified with the following primers: forward (5′-GGATCCAGCTTTATGACCGCAGTAGC-3′), reverse (5′-GCGGCCG-CTCTAGATAGTGGAAGCCCTGTCCTAG-3′) and cloned into *Not*I- and *Bam*HI-restricted pL452 vector harboring a loxP-neo-loxP cassette. Amplification of pL452_Exon11mut with primers containing 60 bp homology to p65 (forward: 5′- ACTGAGCCCG-TGCTCCATGGTTCATCCTCTTCGCTGGCTTTGCAGCTGTAACATGGT GAGAGTACTAACAAAAGCTGGTACCGGGC-3′ and reverse: 5′-CTCCT-GG-AGCAAGAGGGATCTACGTTATGTGAAGGAACCCCACTCCTATTGA-ACCTTTTGGCGGCCGCTCTAGATAGTGGAAGC-3′) was performed to enable the replacement of wild type exon 11 by the mutated exon 11 preceding the loxP-neo-loxP cassette using recombineering [59]. The final *Pvu*I-linearized targeting vector was electroporated into TL1 129Sv/E ES cells. After selection with G418 and expansion, transfectants were tested by Southern Blotting for the presence of NEO;S467A (Fig. 1B). Chimeric mice were produced by microinjection of two independent ES cell targeted clones into C57BL/6 blastocysts. Chimeric males were crossed with C57BL/6 females and these chimeras successfully transmitted the targeted allele. Subsequently, $p65^{+/NEO;S467A}$ mice were crossed with *Hprt*-Cre recombinase mice to excise the NEO cassette. The following primers were used for PCR genotyping on ear DNA of mice used in our studies: forward (5′-GCGTGGCTCACAAGAG-TGAC-3′) and reverse (5′-ACCACCTGACCCAGCTC-TAC-3′) for $p65^{+}$ and $p65^{S467A}$ forward (5′-GCGTGGCTCACAAGAGT-GAC-3′) and reverse (5′-GGCTGCTAAAGCGCATGCT-3′) for $p65^{NEO;S467A}$ forward (5′-GCG-GTCTGGCAGTAAAAACTA-TC-3′) and reverse (5′-ACGAACCTGG

TCGAAATCAGTG-3′) for Cre. The presence of the S467A mutation was confirmed by sequencing of cDNA derived from livers of $p65^{+/+}$ and $p65^{S467A/S467A}$ mice using either the forward (5′-CTGTCTGCACCTGTTCCAAA-3′) or reverse (5′-CTTAGGAGCTGATCTGACTC-3′) primer (Fig. 1D).

4.2. Animal experiments

All mice were backcrossed into C57BL/6 genetic background for at least 5 generations and were housed at a standard 12 h light/dark cycle. Only male mice and wild type littermates as controls were used in this study. All animal-related studies were reviewed and approved by the Animal Care and Use Committee of the University of Groningen. For *in vivo* activation of the NF-κB pathway, mice were injected with either 15 μg/kg mTNFα (R & D Systems, #410-MT) or PBS (control) via the orbital vein and sacrificed at the indicated times. Plasma and various tissues were harvested for further analysis. For high fat feeding studies, male animals were separated and housed individually a week prior to the start of the experiment. Mice were fed a 60% high fat diet *ad lib.* (D12492, DIO Series OpenSource Diets) at the age of 10 weeks till sacrifice. Body weight was measured weekly. After 12 weeks of high fat feeding, body composition was measured using a minispec MRI. Oxygen consumption and energy expenditure were measured using TSE calorimetric cages for 4 consecutive days. After one week of resting period, blood glucose response to oral administration of glucose (1 g/kg)(GTT) or an insulin analog (0.75 U/kg, Novo Rapid Insulin, Bagsvaerd, Denmark)(ITT) was determined. Blood glucose measurements during the GTT and ITT were assessed using OneTouch Select plus glucose meters (LifeScan Benelux, Johnson & Johnson Medical BV) for two h. After 16–18 weeks of high fat feeding, animals were sacrificed using cardiac puncture. Liver and adipose tissue were obtained to perform further experiments.

4.3. Histology

Paraffin embedded sections of tissues (4 μm) were processed by haematoxylin and eosin (H & E) for histological evaluation. Diagnostic classification of NAFLD was performed as described previously [60].

4.4. Generation and culture of MEFs

We intercrossed $p65^{+/S467A}$ mice to derive $p65^{+/+}$, $p65^{+/S467A}$ and $p65^{S467A/S467A}$ MEFs from individual 13.5-day-old fetuses. In short, the uterus was removed from a female that is at day 13.5 of her pregnancy and individual embryos were isolated. The embryonic membrane was removed and stored for genotyping. The head and abdominal organs were removed and the remaining embryo was minced thoroughly using a razor blade. The minced embryo was resuspended in 7 ml of trypsin/EDTA and incubated at 37 °C/15 min, vortexed every 2 min. MEFs were centrifuged at 1500 rpm/5 min, resuspended in Dulbecco's modified Eagle's medium (Gibco, #31966-021; 10% FBS, Hyclone, #SV30160-03; 1× MEM non-essential amino acids, Gibco, #11140-035; Gentamycin 10 μg/ml, Gibco, # 15710-049; 2-Mercaptoethanol 50 μM, Gibco, #31350–010) and seeded in a T75 flask. Cells were frozen at low passages and we used low passage number for the described experiments. For gene expression analyses, 6 independent wild type and homozygous knock-in lines were utilized. We seeded 3×10^5 MEFs per 35-mm dish and activated the NF-κB pathway with 10 ng/ml mTNFα. Cells were harvested in 1 ml QIAzol Lysis Reagent (Qiagen, #79306) at the indicated times. $p65^{+/-}$ and $p65^{-/-}$ immortalized MEFs were kindly provided by Paul Robbins (The Scripps Research Institute, Florida, USA). Wild type control MEFs, either primary or immortalized MEFs, were from the same origin.

4.5. Cell viability

For the cell viability assay, 3 independent wild type and homozygous knock-in immortalized, and one $p65^{+/-}$ MEF lines were used. On day 0, 1×10^5 MEFs per 35-mm dish were seeded for each condition. On day 2, normal medium was replaced by medium containing 0, 25, 50, 75 or 100 ng/ml mTNFα. After 24 h, cells were harvested with trypsin and counted with Tryptan Blue. Relative cell numbers were calculated by setting the number of cells for the condition 0 ng/ml mTNFα at 100% for each MEF line.

4.6. Quantitative real-time PCR

Murine livers and MEFs were homogenized in 1 ml QIAzol Lysis Reagent. Total RNA was isolated by chloroform extraction, precipitated with isopropanol, washed with ethanol and RNA pellets were dissolved in RNase/DNase-free water. Reverse transcription of 0.8-1 μg RNA was performed using the Transcriptor Universal cDNA Master Kit (Roche, #05893151001) according to the protocol provided by the manufacturer. 20 ng cDNA was used for quantitative real-time PCR (qRT-PCR) using FastStart Universal SYBR Green Master (Rox) (Roche, #04913914001) and 7900HT Fast Real-Time PCR System (Applied Biosystems). Data were analyzed with the SDS 2.3 software. Murine adipose tissue was homogenized using Invitrogen TRIzol reagents in order to isolate total RNA by phenol-chloroform extraction. Transcript levels of synthesized cDNA (M-MLV Reverse Transcriptase – Invitrogen – 28,025,013) were measured with Taqman Fast Advanced master mix (Applied Bioscience) on a StepOne Real-Time PCR System (Thermofisher). Ct-values were normalized by a standard curve and controlled by an internal control. As an internal control gene, we used mouse *Cyclophilin A* for MEFs, 18S for liver tissues and 36B4 for adipose tissue. The sequences of the used primers are listed in Supplemental Table 1. The qRT-PCR experiment displayed in Fig. 5 was done by extraction of RNA using the RNeasy Mini Kit (Qiagen, #74106) and QIAShredder columns (Qiagen, #79656). Reverse transcription of 1 μg RNA was performed using the SuperScript II Reverse Transcriptase Kit (Life Technologies, #18064014). cDNA was diluted 10-fold prior to qPCR, which was performed using ABsolute QPCR Mix, SYBR Green, ROX (Thermo Scientific, #AB-1162).

4.7. Quantification of fecal neutral sterols and bile acid

Feces of individually housed animals were collected for 24 h during high fat feeding. Fecal samples were dried at room temperature, thoroughly grinded and 50 mg were used for gas chromatography as described previously [61,62]. Neutral steroids were measured using a 5α-cholestane as internal standard, while bile acids were quantified with the use of 5β-cholanic acid 7α,12α diol. Bile acids and neutral steroids were diluted in heptane and analyzed by GC (Agilent 6890, Amstelveen, the Netherlands) using a CPSil 19 capilliary column (25mx0.25mmx0.2 μm) (Chrompack, Middelburg, The Netherlands).

4.8. Western blotting

Cell extracts were prepared either from cells as described (Renner et al., 2010) or from tissues. These were homogenized in potassium phosphate buffer (25 mM kPi, 500 mM EDTA, 1 mM DTT) supplemented with phosphatase and protease inhibitors and boiled for 10 min. An amount of 30 μg protein was loaded on Tris-HCl Polyacrylamide gel, samples were separated using SDS-PAGE and transferred to PVDF membrane (GE Healthcare, #RPN303F). For Fig. 2A and Fig. S1C, cells were lysed directly in SDS loading buffer. For Figs. 2D, 3 and Fig. S1A, B, cells were washed and scraped in cold PBS and collected by centrifugation. Lysis was performed in NP-40 buffer (20 mM Tris/Hcl pH 7.5, 150 mM NaCl, 10% (v/v) Glycerol, 1% (v/v) NP-40; supplemented with 10 mM NaF, 0.5 mM Na_3VO_4, 0.5 mM

PMSF, 0.5 μg/ml Aprotinin, 0.5 μg/ml Leupeptin prior to use) for 20 min on ice, followed by centrifugation for 10 min at 13.000 rpm and 4 °C. Supernatants were collected in fresh tubes and 5 × SDS loading buffer was added, followed by boiling at 95 °C for 5 min prior to gel loading and Western blotting. All bands were visualized using the ChemiDocTM XRS + System (Bio-Rad Laboratories BV). The various antibodies used for immunoblotting are listed in Table S2.

4.9. Subcellular fractionation

Cells were washed and scraped in cold PBS and collected by centrifugation. Pellets were resuspended in 200 μl buffer A (10 mM Hepes pH 7.9, 10 mM KCl, 0,1 mM EDTA, 0,1 mM EGTA, 1 mM β-Mercaptoethanol, 0.5 mM PMSF) and incubated for 10 min on ice. After addition of NP-40 in a final concentration of 0,25% (v/v), samples were vortexed for 5 s and centrifuged for 10 s at 13.000 rpm. The supernatants representing the cytoplasmic fraction were collected in fresh tubes. The remaining pellets were washed twice in 1 ml buffer A and cleared by centrifugation at 13.000 rpm for 10 s. For preparation of nuclear extracts, pellets were resuspended in 50 μl buffer B (20 mM Hepes pH 7.9, 400 mM NaCl, 1 mM EDTA, 1 mM EGTA, 1 mM β-Mercaptoethanol, 0.5 mM PMSF) and incubated on ice for 20 min, while being agitated several times. After centrifugation at 13.000 rpm for 10 min, supernatants corresponding to the nuclear fraction were collected in fresh tubes. The remaining pellet represents the insoluble chromatin fraction, which was lysed upon addition of 2 × SDS-sample buffer and sonication. All fractions were analyzed by Western blotting.

4.10. Immunoprecipitation of radioactively labeled p65

For pulse experiments cells were trypsinized and washed twice in PBS. Afterwards they were resuspended in DMEM without cysteine and methionine and incubated at 37 °C for 45 min. 300 μ Ci of ^{35}S–labelled cysteine and methionine (EXPRE^{35}S^{35}S Protein Labeling Mix; Perkin Elmer) were added for the indicated time points. Protein synthesis was stopped by scraping the cells into PBS containing 15 μg/ml cycloheximide. Cells were pelleted and resuspended in NP-40 buffer (20 mM Tris/Hcl pH 7.5, 150 mM NaCl, 10% (v/v) Glycerol, 1% (v/v) NP-40; supplemented with 10 mM NaF, 0.5 mM Na_3VO_4, 0.5 mM PMSF, 0.5 μg/ml Aprotinin, 0.5 μg/ml Leupeptin, 10 μg/ml cycloheximide prior to use). After incubation on ice for 20 min, lysates were cleared by centrifugation. 10% of the supernatants were collected as input. The rest of the supernatant was subjected to pre-clearing by adding 30 μl Protein G Plus/Protein A-Agarose (Merck Millipore) and 1 μg anti-rabbit-IgG-antibody for 2 h at 4 °C on a spinning wheel. After short centrifugation the supernatant was transferred to a new tube and incubated with 2 μg anti-p65 antibody (C-20) over night at 4 °C. 30 μl Protein G Plus/Protein A-Agarose was added and the reaction was incubated for 2 h at 4 °C. Beads were washed 3 times with 1 ml NP-40 buffer and finally boiled with 30 μl 1,5 × SDS-sample buffer at 95 °C for 5 min. Samples were separated using SDS-PAGE, gels were dried for 80 min at 80 °C. Radioactivity was visualized using X-ray films. Quantification was carried out using Image Studio Lite 5.2 by LI-COR Biosciences. Signal intensities of the p65-bands and a defined area of the input were acquired. The p65 intensity values were then calculated as percentage of the corresponding input intensity values.

4.11. Chromatin-immunoprecipitation

Cells were washed 2 times with PBS and fixed in a 2 mM DSG solution for 45 min. After 2 washes with PBS, 1% Formaldehyde was added and incubated for 7 min. Formaldehyde was neutralized by addition of Glycine followed by 3 min incubation. Cells were transferred to ice and washed 2 times with ice cold PBS. They were scraped and collected via centrifugation at 1500 rpm for 10 min at 4 °C. Lysis was performed for 20 min on ice in ChIP-RIPA-buffer (10 mM Tris pH 7.5, 150 mM NaCl, 1% (v/v) NP-40, 1% (w/v) Desoxycholate, 0,1% (w/v) SDS, 1 mM EDTA, 1 mM PMSF, 0.5 μg/ml Aprotinin, 0.5 μg/ml Leupeptin, 1 mM DTT). Sonification was carried out with a Covaris S220-sonicator. Cellular debris was removed via centrifugation at 13.000 rpm for 15 min at 4 °C. Supernatants were collected and pre-cleared with protein-A/G-agarose-beads (Millipore #IP10) for 1 h at 4 °C. After removal of the beads and 10% of the volume as the input sample, antibodies were added (3 μg each; rabbit anti-p65 (C-20) (Santa Cruz #sc-372), rabbit anti-IgG (Cell Signaling #2729) and incubated at 4 °C overnight. Protein-A/G-agarose-beads were added for 2 h at 4 °C. Beads were washed twice in ChIP-RIPA-buffer, once in High-Salt-buffer (10 mM Tris pH 7.5, 2 M NaCl, 1% (v/v) NP-40, 0,5% (w/v) Desoxycholate, 1 mM EDTA), once in ChIP-RIPA-buffer and once in TE-buffer (10 mM Tris pH 7.5, 1 mM EDTA). All these steps were carried out at 4 °C. Elution took place at 30 °C for 15 min in 50 μl elution buffer (10 mM Tris pH 7.5, 1 mM EDTA, 1% (w/v) SDS) and was repeated three times, eluates were pooled. From now on, input samples were treated equally to the IP-samples. For reversion of cross-linking, NaCl (final concentration 200 mM) and RNase A (final concentration 0,5 μg/ml) were added and incubated for 30 min at 37 °C. Proteinase K (final concentration 0,5 mg/ml) was added and incubated for 7 h at 37 °C, followed by incubation at 65 °C for 7 h. Chromatin was purified with the Nucleo-Spin Gel and PCR-Clean-Up kit (Macherey and Nagel, # 740609.250) using NTB-buffer (Macherey and Nagel, # 740595.150). Purified chromatin was directly subjected to qPCR.

4.12. Statistical analysis

Statistical analysis was performed using Prism (GraphPad Software) and the unpaired Student's *t*-test, or One-Way ANOVA.

Supplementary data to this article can be found online at http://dx.doi.org/10.1016/j.bbamcr.2017.07.005.

Transparency document

The http://dx.doi.org/10.1016/j.bbamcr.2017.07.005 associated with this article can be found, in online version.

Acknowledgements

We would like to dedicate this paper to Marten Hofker, who passed away during finalizing this manuscript. We thank Paul Robbins for the generous gift of the $p65^{+/-}$ and $p65^{-/-}$ MEFs. This manuscript is supported by the Noaber Foundation, the Graduate School for Drug Exploration (GUIDE), and the University of Groningen. The lab of MLS is supported by grants from the Deutsche Forschungsgemeinschaft (SCHM 1417/8-3, SFB/TRR81, SFB1213, EXC147/1) and Deutsche Krebshilfe (111447).

References

[1] M.S. Hayden, A.P. West, S. Ghosh, NF-kappaB and the immune response, Oncogene 25 (2006) 6758–6780.
[2] M.S. Hayden, S. Ghosh, Shared principles in NF-kappaB signaling, Cell 132 (2008) 344–362.
[3] R.F. Johnson, N.D. Perkins, Nuclear factor-κB, p53, and mitochondria: regulation of cellular metabolism and the Warburg effect, Trends Biochem. Sci. 37 (2012) 317–324.
[4] S. Shalapour, M. Karin, Immunity, inflammation, and cancer: an eternal fight between good and evil, J. Clin. Invest. 125 (2015) 3347–3355.
[5] J.S. Tilstra, C.L. Clauson, L.J. Niedernhofer, P.D. Robbins, NF-κB in Aging and Disease, Aging Dis. 2 (2011) 449–465.
[6] L. Tornatore, A.K. Thotakura, J. Bennett, M. Moretti, G. Franzoso, The nuclear factor kappa B signaling pathway: integrating metabolism with inflammation, Trends Cell Biol. 22 (2012) 557–566.
[7] A.A. Beg, A.S. Baldwin, The I kappa B proteins: multifunctional regulators of Rel/NF-kappa B transcription factors, Genes Dev. 7 (1993) 2064–2070.
[8] M.S. Hayden, S. Ghosh, NF-κB, the first quarter-century: remarkable progress and outstanding questions, Genes Dev. 26 (2012) 203–234.
[9] T. Siggers, A.B. Chang, A. Teixeira, D. Wong, K.J. Williams, B. Ahmed, et al.,

Principles of dimer-specific gene regulation revealed by a comprehensive characterization of NF-κB family DNA binding, Nat. Immunol. 13 (2011) 95–102.
[10] U. Zabel, P.A. Baeuerle, Purified human IκB can rapidly dissociate the complex of the NF-κB transcription factor with its cognate DNA, Cell 61 (1990) 255–265.
[11] S.T. Smale, Hierarchies of NF-κB target-gene regulation, Nat. Immunol. 12 (2011) 689–694.
[12] J. Anrather, G. Racchumi, C. Iadecola, cis-acting, element-specific transcriptional activity of differentially phosphorylated nuclear factor-kappa B, J. Biol. Chem. 280 (2005) 244–252.
[13] F. Christian, E.L. Smith, R.J. Carmody, The regulation of NF-κB subunits by phosphorylation, Cells 5 (2016).
[14] A. Msaki, A.M. Sánchez, L.F. Koh, B. Barré, S. Rocha, N.D. Perkins, et al., The role of RelA (p65) threonine 505 phosphorylation in the regulation of cell growth, survival, and migration, Mol. Biol. Cell 22 (2011) 3032–3040.
[15] N.D. Perkins, Post-translational modifications regulating the activity and function of the nuclear factor kappa B pathway, Oncogene 25 (2006) 6717–6730.
[16] D. Wang, S.D. Westerheide, J.L. Hanson, A.S. Baldwin, Tumor necrosis factor alpha-induced phosphorylation of RelA/p65 on Ser529 is controlled by casein kinase II, J. Biol. Chem. 275 (2000) 32592–32597.
[17] H. Zhong, M.J. May, E. Jimi, S. Ghosh, The phosphorylation status of nuclear NF-kappa B determines its association with CBP/p300 or HDAC-1, Mol. Cell 9 (2002) 625–636.
[18] H. Buss, A. Dörrie, M.L. Schmitz, R. Frank, M. Livingstone, K. Resch, et al., Phosphorylation of serine 468 by GSK-3beta negatively regulates basal p65 NF-kappaB activity, J. Biol. Chem. 279 (2004) 49571–49574.
[19] I. Mattioli, H. Geng, A. Sebald, M. Hodel, C. Bucher, M. Kracht, et al., Inducible phosphorylation of NF-kappa B p65 at serine 468 by T cell costimulation is mediated by IKK epsilon, J. Biol. Chem. 281 (2006) 6175–6183.
[20] R.F. Schwabe, H. Sakurai, IKKbeta phosphorylates p65 at S468 in transactivaton domain 2, FASEB J. 19 (2005) 1758–1760.
[21] H. Geng, T. Wittwer, O. Dittrich-Breiholz, M. Kracht, M.L. Schmitz, Phosphorylation of NF-κB p65 at Ser468 controls its COMMD1-dependent ubiquitination and target gene-specific proteasomal elimination, EMBO Rep. 10 (2009) 381–386.
[22] X. Mao, N. Gluck, D. Li, G.N. Maine, H. Li, I.W. Zaidi, et al., GCN5 is a required cofactor for a ubiquitin ligase that targets NF-κB/RelA, Genes Dev. 23 (2009) 849–861.
[23] R. Moreno, J.M. Sobotzik, C. Schultz, M.L. Schmitz, Specification of the NF-κB transcriptional response by p65 phosphorylation and TNF-induced nuclear translocation of IKK, Nucleic Acids Res. 38 (2010) 6029–6044.
[24] S.-H.E. Tang, F.J. Silva, W.M.K. Tsark, J.R. Mann, A Cre/loxP-deleter transgenic line in mouse strain 129S1/SvImJ, Genesis 32 (2002) 199–202.
[25] A.A. Beg, D. Baltimore, An essential role for NF-kappa B in preventing TNF-alpha -induced cell death, Science 274 (1996) 782–784.
[26] I. Mattioli, A. Sebald, C. Bucher, R.P. Charles, H. Nakano, T. Doi, et al., Transient and selective NF- B p65 serine 536 phosphorylation induced by T cell costimulation is mediated by IκB kinase and controls the kinetics of p65 nuclear import, J. Immunol. 172 (2004) 6336–6344.
[27] F. Renner, M.L. Schmitz, Autoregulatory feedback loops terminating the NF-kappaB response, Trends Biochem. Sci. 34 (2009) 128–135.
[28] E. Mathes, E.L. O'Dea, A. Hoffmann, G. Ghosh, NF-kappaB dictates the degradation pathway of IkappaBalpha, EMBO J. 27 (2008) 1357–1367.
[29] H. Sakurai, H. Chiba, H. Miyoshi, T. Sugita, W. Toriumi, IκB kinases phosphorylate NF-κB p65 subunit on serine 536 in the transactivation domain, J. Biol. Chem. 274 (1999) 30353–30356.
[30] J. Dong, E. Jimi, H. Zhong, M.S. Hayden, S. Ghosh, Repression of gene expression by unphosphorylated NF-kappaB p65 through epigenetic mechanisms, Genes Dev. 22 (2008) 1159–1173.
[31] J. Dong, E. Jimi, C. Zeiss, M.S. Hayden, S. Ghosh, Constitutively active NF-κB triggers systemic TNFα-dependent inflammation and localized TNFα-independent inflammatory disease, Genes Dev. 24 (2010) 1709–1717.
[32] D.J. Van Antwerp, S.J. Martin, T. Kafri, D.R. Green, I.M. Verma, Suppression of TNF-alpha -induced apoptosis by NF-kappa B, Science 274 (1996) 787–789.
[33] M.C. Arkan, A.L. Hevener, F.R. Greten, S. Maeda, Z.-W. Li, J.M. Long, et al., IKK-β links inflammation to obesity-induced insulin resistance, Nat. Med. 11 (2005) 191–198.
[34] D. Cai, M. Yuan, D.F. Frantz, P.A. Melendez, L. Hansen, J. Lee, et al., Local and systemic insulin resistance resulting from hepatic activation of IKK-beta and NF-kappaB, Nat. Med. 11 (2005) 183–190.
[35] X. Zhang, G. Zhang, H. Zhang, M. Karin, H. Bai, D. Cai, Hypothalamic IKKbeta/NF-kappaB and ER stress link overnutrition to energy imbalance and obesity, Cell 135 (2008) 61–73.
[36] S.-H. Chiang, M. Bazuine, C.N. Lumeng, L.M. Geletka, J. Mowers, N.M. White, et al., The protein kinase IKKepsilon regulates energy balance in obese mice, Cell 138 (2009) 961–975.
[37] S. Patel, K. Macaulay, J.R. Woodgett, Tissue-specific analysis of glycogen synthase kinase-3α (GSK-3α) in glucose metabolism: effect of strain variation, PLoS One 6 (2011) e15845.
[38] A. Moles, J.A. Butterworth, A. Sanchez, J.E. Hunter, J. Leslie, H. Sellier, et al., A RelA(p65) Thr505 phospho-site mutation reveals an important mechanism regulating NF-κB-dependent liver regeneration and cancer, Oncogene 35 (2016) 4623–4632.
[39] J.-P. Pradère, C. Hernandez, C. Koppe, R.A. Friedman, T. Luedde, R.F. Schwabe, Negative regulation of NF-κB p65 activity by serine 536 phosphorylation, Sci. Signal. 9 (2016) ra85.
[40] M. Milanovic, M. Kracht, M.L. Schmitz, The cytokine-induced conformational switch of nuclear factor κB p65 is mediated by p65 phosphorylation, Biochem. J. 457 (2014) 401–413.
[41] M. Wickens, P. Anderson, R.J. Jackson, Life and death in the cytoplasm: messages from the 3′ end, Curr. Opin. Genet. Dev. 7 (1997) 220–232.
[42] F. Renner, R. Moreno, M.L. Schmitz, SUMOylation-dependent localization of IKKε in PML nuclear bodies is essential for protection against DNA-damage-triggered cell death, Mol. Cell 37 (2010) 503–515.
[43] B. Kaltschmidt, C. Kaltschmidt, NF-KappaB in long-term memory and structural plasticity in the adult mammalian brain, Front. Mol. Neurosci. 8 (2015) 539.
[44] M. Pelleymounter, M. Cullen, M. Baker, R. Hecht, D. Winters, T. Boone, et al., Effects of the obese gene product on body weight regulation in ob/ob mice, Science 269 (1995) 540–543.
[45] L. Plum, E. Rother, H. Münzberg, F.T. Wunderlich, D.A. Morgan, B. Hampel, et al., Enhanced leptin-stimulated Pi3k activation in the CNS promotes white adipose tissue transdifferentiation, Cell Metab. 6 (2007) 431–445.
[46] A.C. Ribeiro, G. Ceccarini, C. Dupré, J.M. Friedman, D.W. Pfaff, A.L. Mark, Contrasting effects of leptin on food anticipatory and total locomotor activity, PLoS One 6 (2011) e23364.
[47] L. Long, C. Toda, J.K. Jeong, T.L. Horvath, S. Diano, PPARγ ablation sensitizes proopiomelanocortin neurons to leptin during high-fat feeding, J. Clin. Invest. 124 (2014) 4017–4027.
[48] T.V. Berghe, P. Hulpiau, L. Martens, R.E. Vandenbroucke, E. Van Wonterghem, S.W. Perry, et al., Passenger mutations confound interpretation of all genetically modified congenic mice, Immunity 43 (2015) 200–209.
[49] G.S. Hotamisligil, Inflammation and metabolic disorders, Nature 444 (2006) 860–867.
[50] S.E. Shoelson, L. Herrero, A. Naaz, Obesity, inflammation, and insulin resistance, Gastroenterology 132 (2007) 2169–2180.
[51] R.B. Gaynor, M.-J. Yin, Y. Yamamoto, The anti-inflammatory agents aspirin and salicylate inhibit the activity of I(kappa)B kinase-beta, Nature 396 (1998) 77–80.
[52] J.K. Kim, Y.J. Kim, J.J. Fillmore, Y. Chen, I. Moore, J. Lee, et al., Prevention of fat-induced insulin resistance by salicylate, J. Clin. Invest. 108 (2001) 437–446.
[53] H. Hacker, M. Karin, Regulation and function of IKK and IKK-related kinases, Sci. STKE 2006 (2006) re13.
[54] A. Chariot, The NF-kappaB-independent functions of IKK subunits in immunity and cancer, Trends Cell Biol. 19 (2009) 404–413.
[55] M. Aparicio-Vergara, P.P.H. Hommelberg, M. Schreurs, N. Gruben, R. Stienstra, R. Shiri-Sverdlov, et al., Tumor necrosis factor receptor 1 gain-of-function mutation aggravates nonalcoholic fatty liver disease but does not cause insulin resistance in a murine model, Hepatology 57 (2013) 566–576.
[56] R.A. van der Heijden, F. Sheedfar, M.C. Morrison, P.P.H. Hommelberg, D. Kor, N.J. Kloosterhuis, et al., High-fat diet induced obesity primes inflammation in adipose tissue prior to liver in C57BL/6j mice, Aging (Albany NY) 7 (2015) 256–268.
[57] O. Osborn, J.M. Olefsky, The cellular and signaling networks linking the immune system and metabolism in disease, Nat. Med. 18 (2012) 363–374.
[58] A. Moles, A.M. Sánchez, P.S. Banks, L.B. Murphy, S. Luli, L. Borthwick, et al., Inhibition of RelA-Ser536 phosphorylation by a competing peptide reduces mouse liver fibrosis without blocking the innate immune response, Hepatology 57 (2013) 817–828.
[59] L.A. Malureanu, Targeting vector construction through recombineering, Methods Mol. Biol. 693 (2011) 181–203, http://dx.doi.org/10.1007/978-1-60761-974-1_11.
[60] P. Bartuzi, T. Wijshake, D.C. Dekker, A. Fedoseienko, N.J. Kloosterhuis, S.A. Youssef, et al., A cell-type-specific role for murine Commd1 in liver inflammation, Biochim. Biophys. Acta 1842 (2014) 2257–2265.
[61] M. Boesjes, V.W. Bloks, J. Hageman, T. Bos, T.H. van Dijk, R. Havinga, et al., Hepatic farnesoid X-receptor isoforms α2 and α4 differentially modulate bile salt and lipoprotein metabolism in mice, PLoS One 9 (2014) e115028.
[62] J.N. van der Veen, T.H. van Dijk, C.L.J. Vrins, H. van Meer, R. Havinga, K. Bijsterveld, et al., Activation of the liver X receptor stimulates trans-intestinal excretion of plasma cholesterol, J. Biol. Chem. 284 (2009) 19211–19219.